Electronic Supplementary Material (ESI) for Analytical Methods.

Supplementary material

Polychromatic fluorescent MoS_2 quantum dots: fabrication and off-on sensing for fluorine ion in water

Feng-Yi Wu, Ji-Liang Yang, You-Sheng Ye, Ya-Qiong Kong , Rong Wu, Hai-Yan Wang, Xin Wang

Water environment research center, College of Chemistry and Material Engineering, Chaohu University, Hefei 238000, China

Email: wfy@chu.edu.cn

Content

1. Figures and Tables

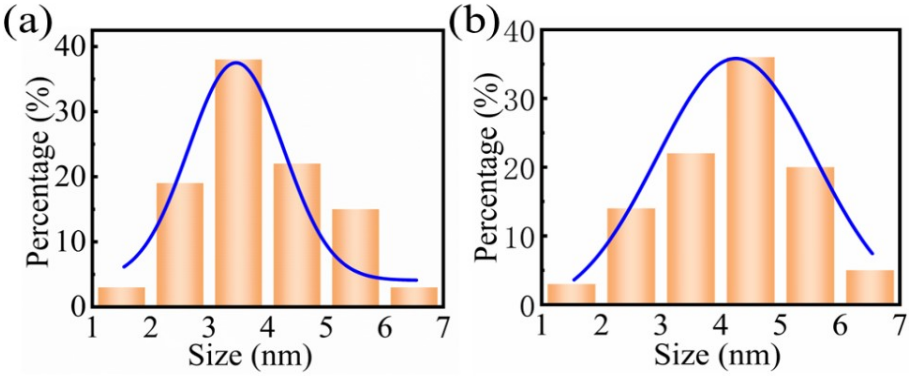

Fig. S1 Size distributions of MoS_2 QDs (a) and I-MoS_2 QDs (b)

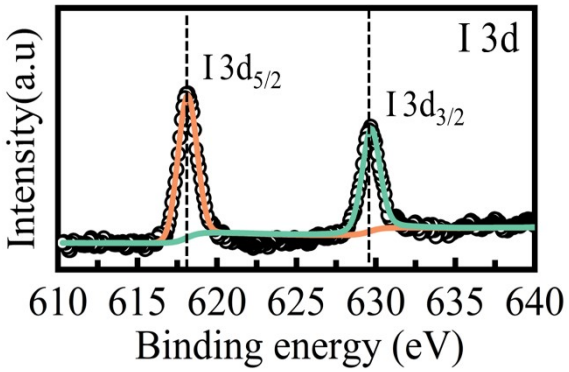

Fig. S2 High-resolution XPS spectra of iodine (I 3d) in I-MoS_2 QDs Binding energies of I $3d_{3/2}$ and I $3d_{5/2}$ are 629.41 and 617.95 eV.

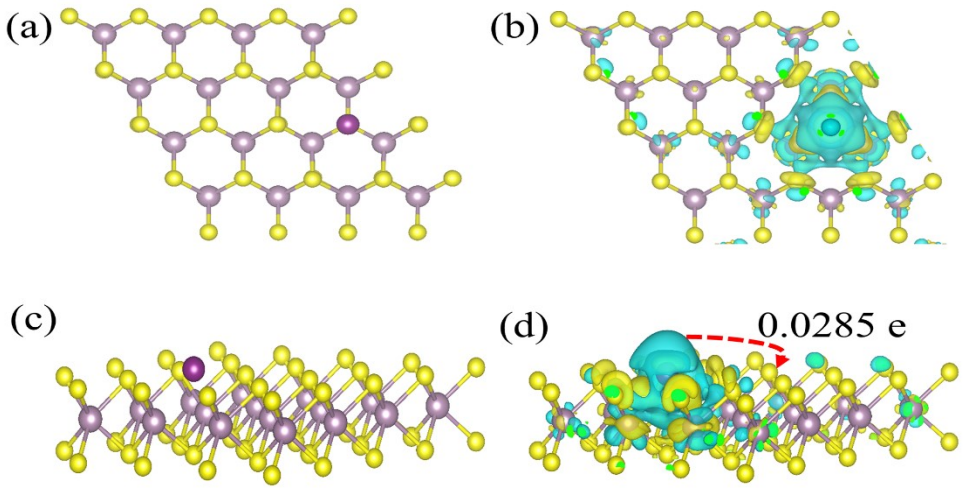

Fig. S3 Optimized geometries for I-MoS_2 QDs in the top (a) and side (c) view (bright

yellow spheres denote S element, lavender spheres: Mo element, purple spheres: I element). Top (b) and side (d) view of charge density difference plots for I-MoS_2 QDs. The khaki and cyan distribution respectively represent electron accumulation and depletion. Isosurface was set as $e^{-1}Å^3$

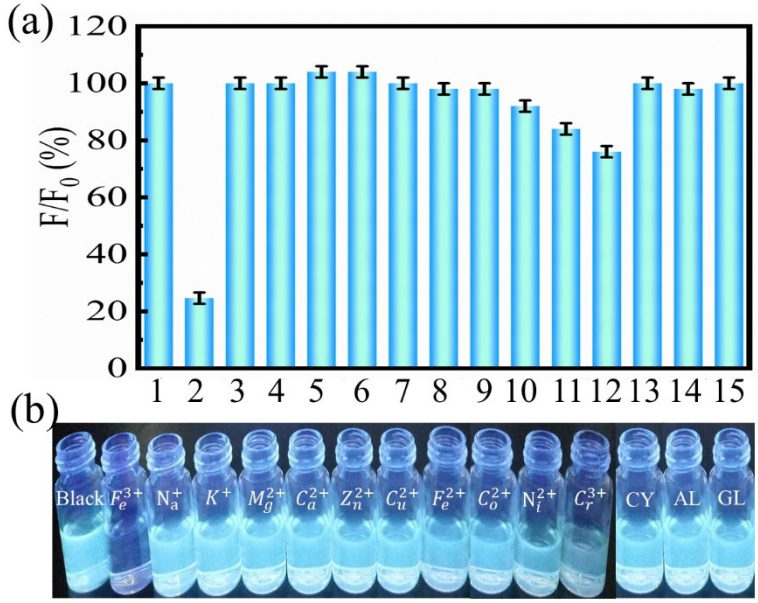

Fig. S4 (a) Relative Fluorescence intensities of I-MoS_2 QDs (10 μM) mixed with different metal ions (250 μM) in aqueous solution. Bars donate the emission intensity ratio F/F_0 (F_0 and F represent the fluorescence intensities of I-MoS_2 QDs without and with different metal ions and the small molecules, 1=blank, 2=Fe^{3+}, 3=Na^+, 4=K^+, 5=Mg^{2+}, 6=Ca^{2+}, 7=Zn^{2+}, 8=Cu^{2+},9= Fe^{2+}, 10=Co^{2+}, 11=Ni^{2+},12=Cr^{3+} ions, 13=L-cysteine (CY), 14=alanine(AL), and 15=glycine(GL)). (b) Under 365 nm UV light, the corresponding pictures of I-MoS_2 QDs without and with different metal ions and the small molecules.

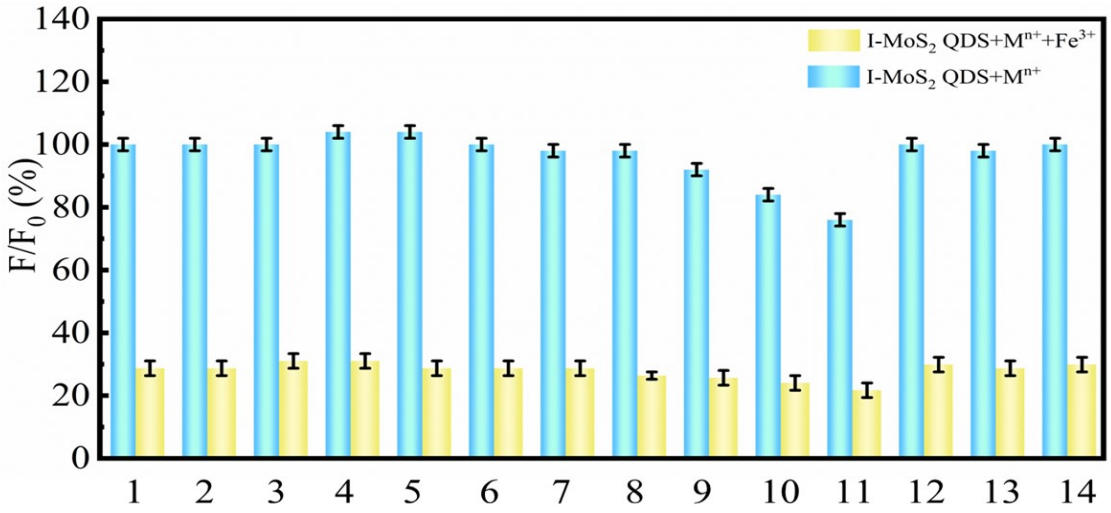

Fig. S5 Interference of different metal ions and small molecules on the detection of Fe^{3+} ions by I-MoS_2 QDs system (1=blank, 2=Na^+, 3=K^+, 4=Mg^{2+}, 5=Ca^{2+}, 6=Zn^{2+}, 7=Cu^{2+},8= Fe^{2+}, 9=Co^{2+}, 10=Ni^{2+},11=Cr^{3+} ions, 12=L-cysteine (CY), 13=alanine(AL), and 14=glycine(GL)).

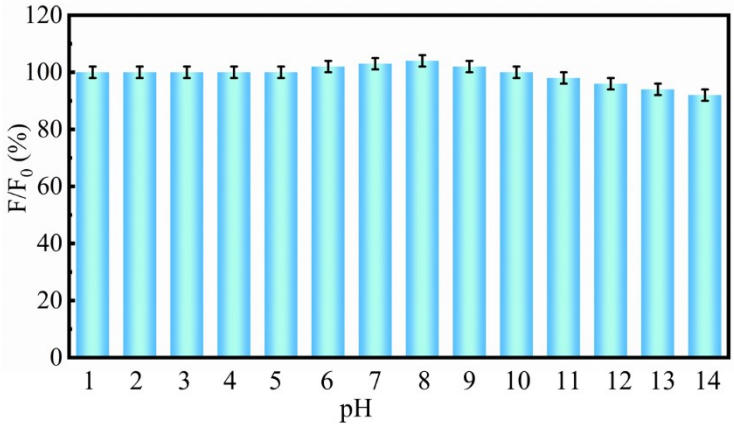

Fig. S6 Change of fluorescence of I-MoS_2 QDs at different pH. (F_0 is the initial fluorescence intensity of the I-MoS_2 QDs. F is fluorescence intensity of the I-MoS_2 QDs at the different pH).

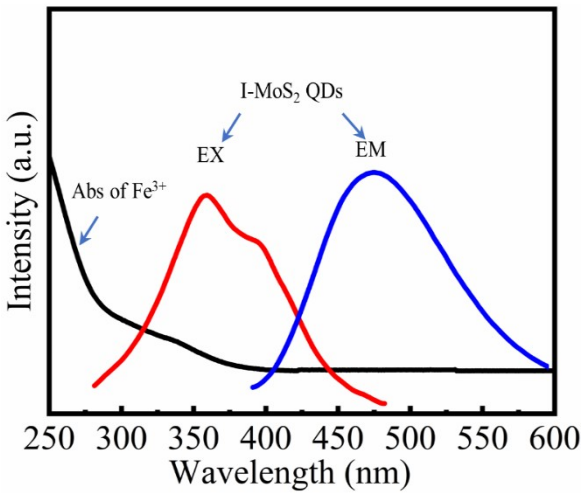

Fig. S7 UV-vis absorbance spectrum of Fe^{3+} ions, the fluorescent excitation (EX) and emission (EM) spectra of N-MoS_2 QDs.

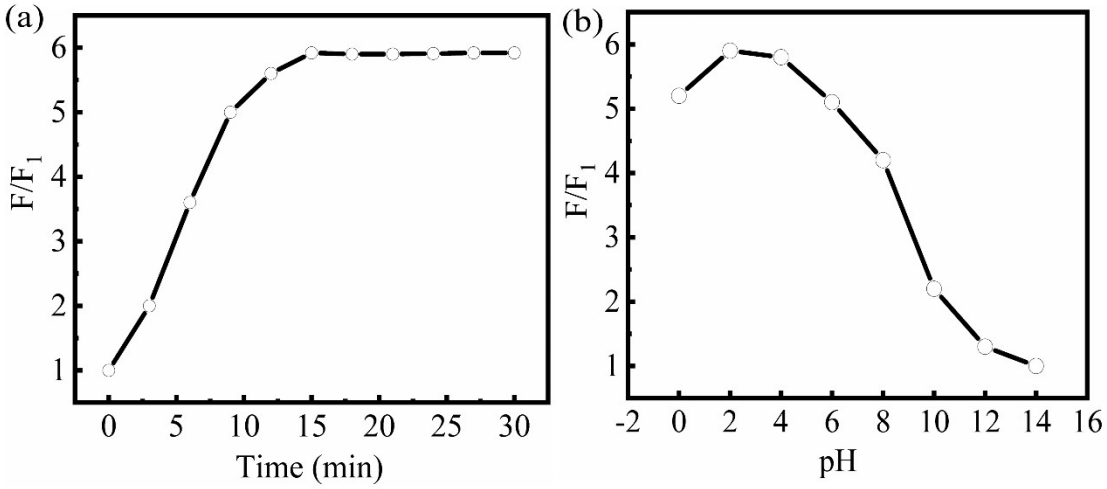

Fig. S8 Fluorescence intensity ratios F/ F_1 versus incubation time (a) and pH (b) after the addition of F^- ions into I-MoS_2 QDs/Fe^{3+}system. F_1 and F is fluorescence intensity of I-MoS_2 QDs/ Fe^{3+} compound before and after adding F^- ions.

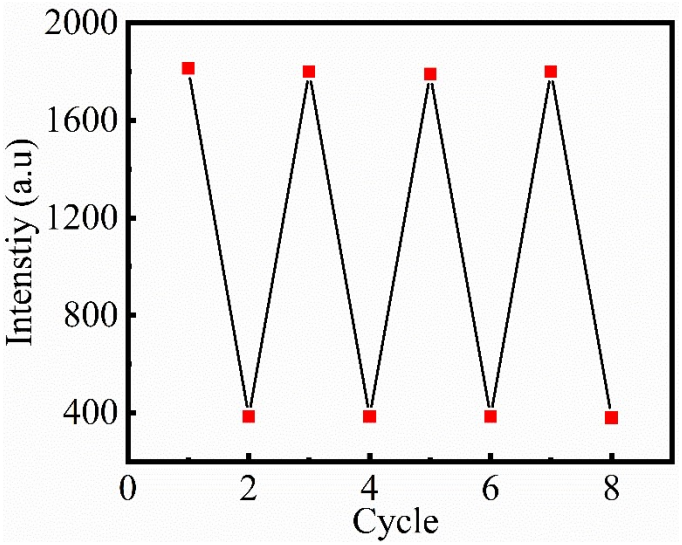

Fig. S9 Fluorescence intensities of "turn-off-on" cycles as alternately addition of Fe^{3+} and F^- ions into I-MoS_2 QDs/Fe^{3+} system.

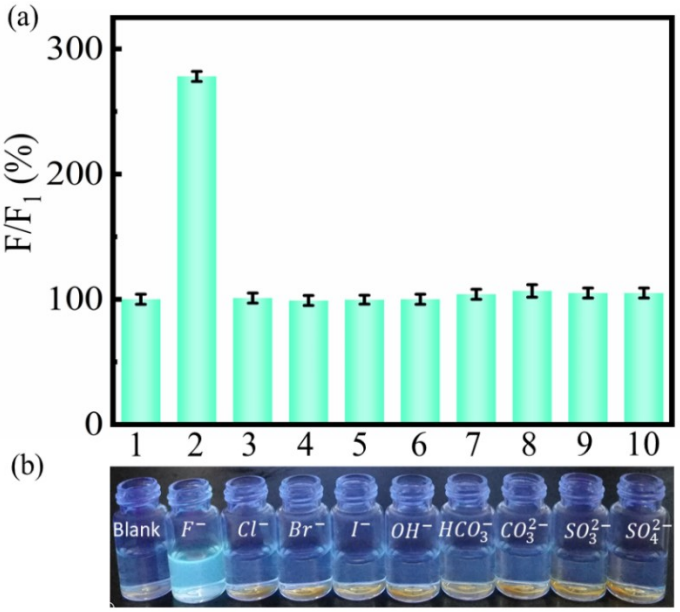

Fig. S10 (a) Relative Fluorescence intensities of 10 μM I-MoS_2 QDs mixed with 250 μM Fe^{3+} aqueous solution without and with various anions. Bars donate the emission intensity ratio F/F_1 (F_1 and F represent fluorescence intensities of I-MoS_2 QDs/ Fe^{3+} system without and with different anions, 1=blank, 2=F^-, 3=Cl^-, 4=Br^-, 5=I^-, 6=OH^-, 7=HCO_3^-, 8=CO_3^{2-}, 9=SO_3^{2-} and 10=SO_4^{2-}). (b) Under 365 nm UV light, the corresponding pictures of I-MoS_2 QDs/Fe^{3+} system without and with different anions.

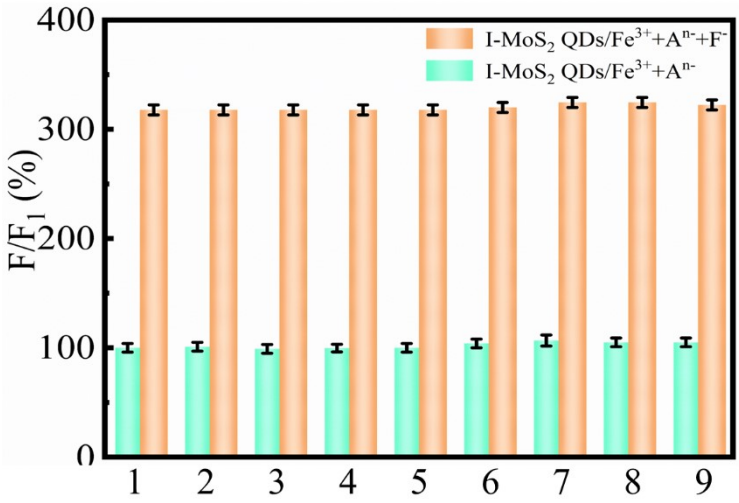

Fig.S11 Interference of different anions on the detection of F^- ions by I-MoS_2 QDs/Fe^{3+} system (1=blank, 2=Cl^-, 3=Br^-, 4=I^-, 5=OH^-, 6=HCO_3^-, 7=CO_3^{2-}, 8=SO_3^{2-} and 9=SO_4^{2-}).

Table S1. Emission wavelengths (nm), FWHM, photoluminescence quantum yield (PLQY) of MoS_2 QDs samples labeled as S1, S2, S3 and S4.

Sample	Emission wavelength (nm)	FWHM (nm)	PLQY (%)
S1	423	95	6.8[a]
S2	474	98	7.1[a]
S3	501	105	6.4[b]
S4	529	110	5.7[b]

[a] Quinoline sulfate as a standard (PLQY = 55%). [b] Rhodamine 6G as a standard (PLQY =95%).

Table S2. Determination of F^- ions by the fluorescent probes based on different quantum dots.

Sensor	Linearity	LOD	Ref.
CdS QDs	10–300 μM	6 μM	1
CdS/ZnS QDs	300–5600 μM	74.0 μM	2
CdTe QDs	0–10 mM	5.0 μM	3
Ag doped CdS/ZnS QDs	10–1200 μM	5.25 μM	4
Se,N-doped C QDs	/	1.3 μM	5

graphitic carbon nitride QDs	10–120 μM	4.06 μM	6
Mn^{2+}-doped ZnTe/ZnSe QDs	0.25–1.5 μM	0.1 μM	7
Fe^{3+}-MoS_2 QDs	2.5-80 μM	1.4 μM	This work

Table S3. Determination of F^- (μM) in three water samples with I-MoS_2 QDs/Fe^{3+} fluorescent probe and ion chromatograph (IC) method (n=3).

Samples	F^- concentration (μM)	found F^- (μM)	Recovery (%)	RSD (%)	Found by IC (μM)
Lake	0	26.20	-	3.1	26.30±0.10
water	5	31.40	97.6	1.5	31.27±0.15
	10	36.50	102.0	2.0	36.40±0.20
Tap	0	20.90	-	2.9	20.50±0.15
water	5	25.34	98.4	1.3	25.44±0.18
	10	30.76	101.9	1.7	30.57±0.15
Well	0	42.3	-	3.9	42.10±0.14
water	5	47.6	103.2	2.8	47.26±0.18
	10	52.2	98.9	1.8	52.09±0.15

2. Formula and calculation

2.1 Photoluminescence quantum yield (PLQY)

PLQY of MoS_2 QDs was tested via a relative measuring method. PLQY of Quinoline sulfate aqueous solution (0.55 in 0.1 M diluted H_2SO_4) and Rhodamine 6G (0.95 in ethanol) were selected as reference materials. Absorbed optical density of the reference materials andMoS_2 QDs were kept under 0.1 to minimize re-absorption effects. The PLQY of MoS_2 QDs was calculated according to the formula:

$$\Phi_s = \Phi_r \times \left(\frac{A_r}{A_s}\right) \times \left(\frac{I_s}{I_r}\right) \times \left(\frac{n_s}{n_r}\right)^2$$

Where Φ_s and Φ_r represent PLQY of MoS_2 QDs samples and reference materials. A_s and A_r stand for absorbance of MoS_2 QDs samples and reference materials. I_s and I_r were integrated emission intensity of MoS_2 QDs samples and reference materials. n_s

and n_r denoted respectively refractive index of solvents used for MoS_2 QDs and reference materials. DI water, ethanol and 0.1 M H_2SO_4 are respectively used to dissolve MoS_2 QDs, Rhodamine 6G and Quinine Sulfate. Refractive index of DI water, ethanol and 0.1 M H_2SO_4 are respectively 1.33, 1.36 and 1.63.

2.2 Computational detail of DFT

DFT calculations were conducted through the Vienna ab initio Simulation Package (VASP) with the projector augment wave method. The exchange-correlation function is treated with the generalized gradient approximation of the PBE functional. A plane-wave cutoff energy was set as 500 eV, and structure relaxation was performed until the convergence criteria of energy and force reached 1×10^{-5} eV and 0.02 eV $Å^{-1}$, respectively. A vacuum layer of 20 Å was constructed to eliminate interactions between periodic structures of surface models. The Brillouin zone was sampled with 4 × 4 × 1 K points for MoS_2 (002) surface.

2.3 The Stern–Volmer equation

$$\frac{F_0 - F}{F} = K_{SV} C_q = K_q \tau_0 C_q$$

Where F_0 and F are the fluorescence-intensities of I-MoS_2 QDs with and without Fe^{3+} ions; C_q is Fe^{3+} ions concentration, and K_{sv} is 0.0114 $(\mu mol/L)^{-1}$ obtained by the slope of the regression line. Here, the τ_0 is average fluorescence-lifetime of MoS_2 QDs about 1.42 ns. As-obtained quenching rate constant K_q is about 8.03×10^{12} $(mol/L)^{-1}s^{-1}$, which is higher than 1.0×10^{10} $(mol/L)^{-1}s^{-1}$.

3. References

[1] S. Liu, H. Wang, Z. Cheng, H. Liu, *Sens. Actuators B-Chem*., 2016,**232**, 306–312.

[2] R.C. Mulrooney, N. Singh, N. Kaur, J.F. Callan, *Chem. Commun*., 2009, 686–688.

[3] J. Liu, X. Yang, K. Wang, R. Yang, H. Ji, L. Yang, C. Wu, A switchable fluorescent quantum dot probe based on aggregation/disaggregation mechanism, *Chem. Commun.* 2011,**47,** 935–937.

[4] S.S. Boxi, S. Paria, Fluorometric selective detection of fluoride ions in aqueous media using ag doped CdS/ZnS core/shell nanoparticles, *Dalton Trans*. 2016,**45**, 811–819.

[5] X. Zhang, X. Tan, Y. Hu, Blue/yellow emissive carbon dots coupled with curcumin: a hybrid sensor toward fluorescence turn-on detection of fluoride ion, *J. Hazard. Mater.,* 2021,**411**,125184–125191.

[6] M. Devi, P. Das, P.K. Boruah, M.J. Deka, R. Duarah, A. Gogoi, D. Neog, H.S. Dutta, M.R. Das, Fluorescent graphitic carbon nitride and graphene oxide quantum dots as efficient nanozymes: colorimetric detection of fluoride ion in water by graphitic carbon nitride quantum dots*, J. Environ. Chem. Eng*., 2021,**9**,104803–104816.

[7] H. Wang, T.-Y. Hu, Z.-T. Zhao, X.-Y. Zhang, Y. Wang, X.Q. Duan, D.-W. Liu, L. Jing, Q. Ma, A novel Mn^{2+}-doped core/shell quantum dot-based intracellular probe for fluoride anions sensing in MC3T3-E1 osteoblastic cells, *Talanta*, 2016, **149**,285–289.